JACS
JOURNAL OF THE AMERICAN CHEMICAL SOCIETY
Communication
pubs.acs.org/JACS

Design and Synthesis of Hydroxide Ion–Conductive Metal–Organic Frameworks Based on Salt Inclusion

Masaaki Sadakiyo,*[,†,‡] Hidetaka Kasai,[‡,§] Kenichi Kato,[‡,§] Masaki Takata,[§] and Miho Yamauchi*[,†,‡,∥]

[†]International Institute for Carbon Neutral Energy Research (WPI-I2CNER), Kyushu University, 744 Moto-oka, Nishi-ku, Fukuoka 819-0395, Japan

[‡]CREST, JST, 4-1-8 Honcho, Kawaguchi, Saitama 332-0012, Japan

[§]RIKEN SPring-8 Center, 1-1-1 Kouto, Sayo-cho, Sayo-gun, Hyogo 679-5148, Japan

[∥]Department of Chemistry, Faculty of Science, Kyushu University, 6-10-1 Hakozaki, Higashi-ku, Fukuoka 812-8581, Japan

Supporting Information

ABSTRACT: We demonstrate a metal–organic framework (MOF) design for the inclusion of hydroxide ions. Salt inclusion method was applied to an alkaline-stable ZIF-8 (ZIF = zeolitic imidazolate framework) to introduce alkylammonium hydroxides as ionic carriers. We found that tetrabutylammonium salts are immobilized inside the pores by a hydrophobic interaction between the alkyl groups of the salt and the framework, which significantly increases the hydrophilicity of ZIF-8. Furthermore, ZIF-8 including the salt exhibited a capacity for OH^- ion exchange, implying that freely exchangeable OH^- ions are present in the MOF. ZIF-8 containing OH^- ions showed an ionic conductivity of 2.3×10^{-8} S cm^{-1} at 25 °C, which is 4 orders of magnitude higher than that of the blank ZIF-8. This is the first example of an MOF-based hydroxide ion conductor.

Ionic conductors are key materials for the construction of energy conversion and storage devices such as secondary batteries and fuel cells.[1] Recently, hydroxide ion conductors have received a great deal of interest as electrolytes for alkaline fuel cells that can operate without precious-metal catalysts.[2] Liquid electrolytes[3] and organic polymers[2,4] have mainly been used in the alkaline fuel cells developed so far. Regardless of the many advantages of crystalline solids in terms of thermal stability, high regularity, and structural visualization, such materials have not been studied as much as hydroxide ion conductors[5] because of the low designability of inorganic solids for constructing various architectures.

Metal–organic frameworks (MOFs) have emerged as designable crystalline solids that can achieve various functionalities such as gas storage,[6] separation,[7] controlled delivery,[8] catalysis,[9] magnetism,[10] and electrical conductivity.[11] In the past 5 years, MOF-based proton conductors have been widely studied by constructing various conduction pathways using proton carriers inside the framework;[12] this indicates that MOFs have a high potential to be applied as building blocks for the construction of ion conductors. Hydroxide ion conduction in MOFs, however, has not been achieved to date.

In general, hydroxide ion conduction at ambient temperature requires OH^- ion carriers and conducting pathways composed of hydrogen-bonding networks,[2] as is the case for proton conduction.[1c,13] Kitagawa et al.[12a] have reported basic designs for introducing proton carriers into MOFs. Considering OH^- ions are opposite in charge to H^+ (H_3O^+) ions, there are two approaches to introducing OH^- ions into MOFs that can be described by analogy to those for proton conductors: OH^- ions are inserted as counteranions into the pores (type A, corresponds to types I and II for proton conductors[12a]) or hydroxide salts are incorporated into the voids (type B, corresponds to type III[12a]). It is important to consider the stability of the frameworks for a strong base of OH^- ions.

In this work, we propose a rational approach to synthesize MOFs that include OH^- ions based on "salt inclusion into alkaline-stable MOFs" (that is, type B). There are two prerequisites for the reaction: an alkaline-stable porous MOF is used as the mother framework, and cations having an affinity to adsorb to the frameworks must be employed. We thus chose ZIF-8 (ZIF = zeolitic imidazolate framework; Figure 1a,b)[14] as the mother framework, which is highly stable for Lewis bases.[14a,15] Considering that the hydrophobic pore surface inside ZIF-8 is produced as a result of the presence of a methyl group on the ligands,[14d] *n*-tetrabutylammonium hydroxide salt, NBu_4OH (Bu = *n*-butyl), containing alkyl groups was selected as the included salt. The alkylammonium cations are likely to be immobilized inside the pores through a hydrophobic interaction between the alkyl groups and the hydrophobic framework in ZIF-8 (Figure 1c). Here, we report the successful production of a novel MOF containing hydroxide ions, $(NBu_4)_m(A)_n\{Zn(mim)_2\}_6$ (Hmim = 2-methylimidazole; A^- = hydrocarbonate (abbreviated here as NBu_4-ZIF-8) and hydroxide ions (NBu_4-ZIF-8-OH)). The NBu_4^+ ions are sufficiently immobilized in ZIF-8 for the MOF to retain OH^- ions. We were able to confirm that including the hydroxide salt enhanced the ionic conductivity by 4 orders of magnitude.

NBu_4-ZIF-8 was prepared by mixing ZIF-8 and an aqueous solution of NBu_4OH (details are given in the Supporting Information). ZIF-8 was synthesized by mixing a methanol solution of $Zn(NO_3)_2{\cdot}6H_2O$ and 2-methylimidazole, in accordance with a procedure reported previously.[14c] Elemental analysis revealed that NBu_4-ZIF-8 has 0.70 ion pairs per ZIF-8

Received: October 9, 2013
Published: January 14, 2014

   dx.doi.org/10.1021/ja410368j | J. Am. Chem. Soc. 2014, 136, 1702–1705

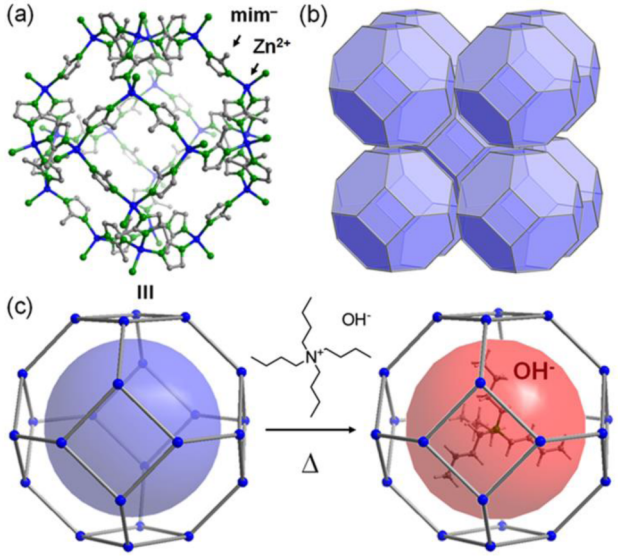

Figure 1. Representation of the crystal structure of ZIF-8[14a] and a schematic image of the salt inclusion: (a) cage and (b) 3-D porous SOD structures of ZIF-8. (c) Schematic view of the preparation procedure for NBu_4-ZIF-8-OH.

cage and that the OH^- ions in the MOF are possibly converted to HCO_3^- ions because of the absorption of CO_2 from the air. The infrared spectrum of NBu_4-ZIF-8 exhibited CH stretching modes of the butyl groups, which are not derived from ZIF-8, at 2961 and 2876 cm^{-1}, indicating the presence of NBu_4^+ ions (Figure S1, Supporting Information). To eliminate the possibility that NBu_3 molecules are derived from Hofmann elimination,[16] a decomposition reaction of NR_4OH to give NR_3 molecules, we examined the structure of the included cations by measuring the ^1H NMR spectra of NBu_4-ZIF-8 dissolved in D_2O/D_2SO_4 (9/1).[17] We could not recognize any signals assignable to $NHBu_3^+$ in the spectra (Figure S2, Supporting Information), which ruled out the presence of NBu_3 molecules in ZIF-8. A thermogravimetric analysis of NBu_4-ZIF-8 revealed weight loss at 127 °C, which is attributable to the desorption of 1-butene, H_2O, and CO_2 derived from the decomposition of NBu_4HCO_3 to give NBu_3 (Figure S3, Supporting Information). These molecules were detected by temperature-programmed desorption mass spectrometry at mass numbers of 18 (i.e., H_2O), 44 (CO_2), and 56 (C_4H_8) (Figure S4, Supporting Information). These results confirm the stability of the salt inclusion state up to 120 °C. It should be noted that the included salt could not be removed by further washing with water, even though water is a good solvent for this salt, implying that the guest salts are trapped through a strong hydrophobic interaction with the framework. The hydrophilic counteranions, however, are likely to be exchangeable.

To clarify the crystal structure of NBu_4-ZIF-8, we conducted in-house X-ray powder diffraction (XRPD) measurements (Figure S5, Supporting Information). The diffraction pattern of NBu_4-ZIF-8 appeared to be fundamentally the same as that of the starting ZIF-8, indicating that the framework structure of ZIF-8 does not decompose when the reaction proceeds under strongly alkaline conditions (pH >14). There were, however, apparent differences in the relative intensities of the ZIF-8 and NBu_4-ZIF-8 spectra; the atomic arrangement in ZIF-8 is modified by the salt inclusion without any change to the crystal symmetry. This strongly suggests the presence of guest salts in the pore space of ZIF-8. To obtain direct evidence of this, we performed an electron density visualization by means of maximum entropy method (MEM)−Rietveld analysis[18a] using synchrotron XRPD data obtained on the RIKEN materials science beamline BL44B2[18b] at SPring-8 (details are given in the Supporting Information). Figure 2 shows the isodensity

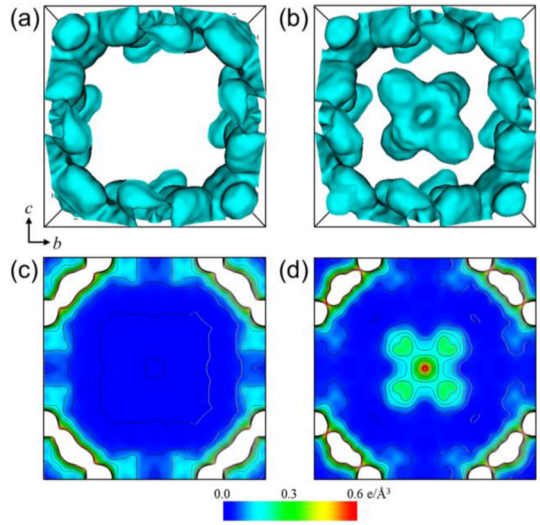

Figure 2. Electron density distribution derived from the synchrotron XRPD data of ZIF-8 and NBu_4-ZIF-8: isodensity (0.15 e $Å^{-3}$) surface maps of (a) ZIF-8 and (b) NBu_4-ZIF-8 and contour maps in the (200) plane of (c) ZIF-8 and (d) NBu_4-ZIF-8. Contour lines are drawn from 0.01 to 0.70 e $Å^{-3}$ at intervals of 0.05 e $Å^{-3}$.

surface and contour maps of ZIF-8 and NBu_4-ZIF-8. As shown in Figure 2a,c for ZIF-8, no charge localization was observed in the pore. In contrast, additional charge was found around the cage center in NBu_4-ZIF-8. From these results, we concluded that ZIF-8 encapsulates the NBu_4HCO_3 salts inside the pore. Judging from the pore diameter of 11.6 Å,[14a] there should be some extra space between ZIF-8 and the NBu_4HCO_3 salts. We conducted nitrogen gas adsorption measurements at 77 K to verify this assumption (Figure S7 (left), Supporting Information) and found that the surface area of ZIF-8 (1664 $m^2\ g^{-1}$; BET) was reduced by 52% (61%, calculated on the basis of units of $m^2\ mol^{-1}$) to 871 $m^2\ g^{-1}$ (BET) by the salt inclusion. Considering that 30% of the cages were not occupied by the salt, guest-accessible space is thought to remain even in salt-occupied cages.

To examine the anion exchange ability for OH^- ions, we induced an ion-exchange reaction by stirring NBu_4-ZIF-8 powder in NaOH aqueous solution (see the Supporting Information) and estimated the amount of OH^- ion adsorption using CO_2 gas adsorption measurements. Figure 3 shows the CO_2 adsorption isotherms of the ion-exchanged sample (NBu_4-ZIF-8-OH) at 298 K. There is a clear difference between the isotherms of NBu_4-ZIF-8-OH and NBu_4-ZIF-8, and judging by the linear increase in the adsorption with pressure, CO_2 is physically adsorbed in NBu_4-ZIF-8. Above 0.2 kPa, the adsorption curve of NBu_4-ZIF-8-OH follows the same trend as that of NBu_4-ZIF-8, suggesting that the porous structure of NBu_4-ZIF-8 does not change with the reaction. NBu_4-ZIF-8-OH was found to absorb CO_2 in low-pressure regions (less than 0.2 kPa), and the increase in the adsorption is assigned to the chemisorption of CO_2 resulting from the neutralization of OH^- ions: i.e., the formation of HCO_3^- ions. The observed

dx.doi.org/10.1021/ja410368j | J. Am. Chem. Soc. 2014, 136, 1702−1705

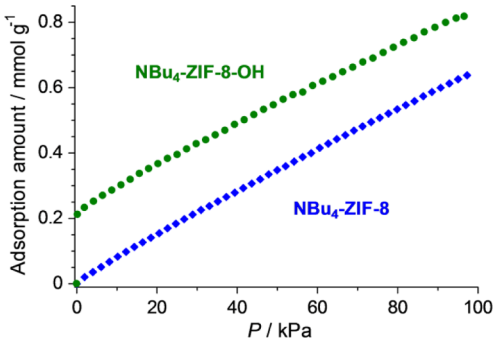

Figure 3. CO_2 adsorption isotherms of NBu_4-ZIF-8 (blue) and NBu_4-ZIF-8-OH (green) at 298 K.

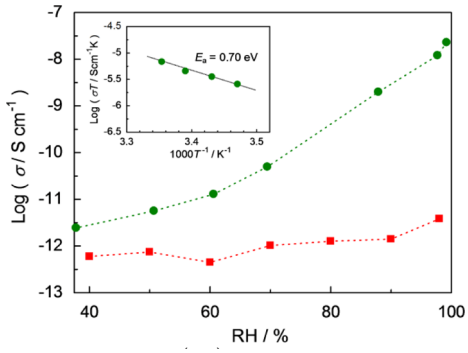

Figure 4. Relative humidity (RH) dependence of the ionic conductivity (25 °C). Green circles and red squares correspond to NBu_4-ZIF-8-OH (under N_2 conditions) and ZIF-8, respectively. The inset shows an Arrhenius plot of the conductivity of NBu_4-ZIF-8-OH (RH is over 96%).

increase corresponds to a replacement of 47% of the initially included HCO_3^- ions by OH^- ions and 0.21 mmol g^{-1} of the OH^- concentration in NBu_4-ZIF-8-OH. To the best of our knowledge, this is the first example of an MOF including free OH^- ions. Other anions included in NBu_4-ZIF-8-OH are likely to be HCO_3^- or CO_3^{2-} ions. According to the acidity of HCO_3^- (pK_{a2} = 10.3), we hypothesize that divalent CO_3^{2-} ions form in the pores during the exchange reaction (pH >14) and are more strongly adsorbed to the framework than the monovalent HCO_3^- ions. The existence of CO_3^{2-} ions probably prevents complete anion exchange to OH^- ions. Furthermore, elemental analysis revealed that there is no significant difference between the contents of NBu_4^+ ions before and after the ion exchange, indicating that the cations were not exchanged through this procedure (see the Supporting Information). Note that we could not observe CO_2 chemisorption for blank ZIF-8 even after treatment in NaOH aqueous solution, which suggests that ZIF-8 does not have the capacity for OH^- ion inclusion. As shown in Figure S7 (Supporting Information), the surface area of NBu_4-ZIF-8-OH (868 m^2 g^{-1}) was almost the same as that of NBu_4-ZIF-8 (871 m^2 g^{-1}), indicating that there is no remarkable change in the porous structure. This also indicates that the cations are bound stably by the framework of ZIF-8.

We found that the included OH^- ions are exchangeable. To evaluate the effect of the included hydroxide salts on the ionic conductivity, we performed ac impedance measurements using compacted pellets of the powdered sample. All of the NBu_4-ZIF-8-OH measurements were performed under nitrogen gas conditions to avoid the absorption of CO_2 from the air. The ionic conductivities of NBu_4-ZIF-8-OH and ZIF-8 were determined to be 2.3×10^{-8} S cm^{-1} (99% RH) and 3.8×10^{-12} S cm^{-1} (98% RH) at 25 °C, respectively (Figure 4 and Figure S8 (Supporting Information)). Considering that the framework structure of NBu_4-ZIF-8-OH is the same as that of ZIF-8, the observed enhancement in the ionic conductivity of 4 orders of magnitude can be attributed to the included salt. The ionic conductivity of NBu_4-ZIF-8-OH increases with RH, suggesting that the conductivity is not enhanced by the diffusion of aprotic NBu_4^+ ions but by the diffusion of hydrogen-bonding species of OH^- ions. Therefore, we think that the structure of the adsorbed water molecules in NBu_4-ZIF-8-OH is strongly related to the ion-conducting pathways. We measured water vapor adsorption isotherms of ZIF-8 before and after the salt inclusion (Figure S9, Supporting Information) and found a remarkable difference between NBu_4-ZIF-8-OH and ZIF-8. NBu_4-ZIF-8-OH showed a larger amount of water adsorption, even though it has a smaller surface area. This means that the hydrophobic character of ZIF-8 becomes hydrophilic after the salt inclusion. We believe that both the electrostatic and hydrogen-bonding interactions derived from the included ions might play an important role in the adsorption of water molecules.[19] We also found that NBu_4-ZIF-8 exhibits 1 order higher conductivity (6.2×10^{-7} S cm^{-1}, 98% RH, 25 °C) in comparison with that of NBu_4-ZIF-8-OH, while both inclusion compounds contain almost identical amounts of NBu_4^+ ions. This clearly indicates that the ionic conductivity is mainly derived from the anionic species. A charge-migration model of hydrated OH^- ions has been proposed as a transportation mechanism of OH^- ions in water.[13] Charge on the OH^- ions migrates efficiently through proton transfer from neighboring water molecules through hydrogen-bonding networks, which is similar to the case of hydrated H_3O^+ ions (Grotthuss mechanism[20]), as shown by the anomalously high mobility of OH^- ions in aqueous solution in comparison with those of other anions.[13,21] This indicates that the formation of hydrogen-bonding networks of OH^- and water molecules can enhance the OH^- ion conductivity. Therefore, we suppose that the increase in the conductivity of NBu_4-ZIF-8-OH with humidity occurs by such a migration of OH^- ions in the pores of ZIF-8. However, the conducting mechanism of this material is still under investigation. The temperature dependence of the ionic conductivity, shown in the Arrhenius plot in the inset of Figure 4, gives an estimated activation energy E_a of 0.70 eV. This E_a value is much higher than that of hydrated OH^- ions in liquid (less than 0.2 eV)[22] and suggests that there are some unfavorable features in the conducting pathways (e.g., small apertures in ZIF-8 (3.4 Å in diameter)).[14a] Clarification of the relationship between the frame structure and the OH^- ion conductivity in various MOFs is expected to provide further enhancement of the OH^- ion conductivity in solids.

In summary, we have proposed a design for novel OH^- ion conductive MOFs and have synthesized a novel MOF that includes OH^- ions by employing salt inclusion in alkaline-stable MOFs. The hydroxide salts were successfully immobilized in ZIF-8, and the MOF has the capacity for OH^- ion inclusion. This is the first example of an MOF including freely exchangeable OH^- ions, which behave as carriers for ion conduction. We have demonstrated the potential of the salt inclusion to enhance ionic conductivity. Further, the chemical characteristics of the pores in ZIF-8 were controlled by the salt

dx.doi.org/10.1021/ja410368j | J. Am. Chem. Soc. 2014, 136, 1702−1705

inclusion successfully. We believe that this technique will be widely applicable to the functionalization of MOFs.

■ ASSOCIATED CONTENT

Supporting Information

Text, figures, tables, and a CIF file giving details of the syntheses, compound characterizations, physical measurements, and X-ray crystallographic data. This material is available free of charge via the Internet at http://pubs.acs.org.

■ AUTHOR INFORMATION

Corresponding Author

sadakiyo@i2cner.kyushu-u.ac.jp; yamauchi@i2cner.kyushu-u.ac.jp

Notes

The authors declare no competing financial interest.

■ ACKNOWLEDGMENTS

This work was partially supported by the JST-CREST and JSPS KAKENHI Grant Nos. 24850013, 24655040, and 25288030. The synchrotron radiation experiments were performed on the BL44B2 beamline in SPring-8 with the approval of RIKEN (Proposal No. 20130091).

■ REFERENCES

(1) (a) Meyer, W. H. *Adv. Mater.* **1998**, *10*, 439−448. (b) Knauth, P. *Solid State Ionics* **2009**, *180*, 911−916. (c) Kreuer, K. D.; Paddison, S. J.; Spohr, E.; Schuster, M. *Chem. Rev.* **2004**, *104*, 4637−4678.

(2) (a) Asazawa, K.; Yamada, K.; Tanaka, H.; Oka, A.; Taniguchi, M.; Kobayashi, T. *Angew. Chem., Int. Ed.* **2007**, *46*, 8024−8027. (b) Lan, R.; Tao, S. *Electrochem. Solid-State Lett.* **2010**, *13*, B83−B86.

(3) Gülzow, E. *J. Power Sources* **1996**, *61*, 99−104.

(4) (a) Varcoe, J. R.; Slade, R. C. T. *Fuel Cells* **2005**, *5*, 187−200. (b) Pan, J.; Chen, C.; Zhuang, L.; Lu, J. *Acc. Chem. Res.* **2012**, *45*, 473−481.

(5) (a) Hibino, T.; Shen, Y.; Nishida, M.; Nagao, M. *Angew. Chem., Int. Ed.* **2012**, *51*, 10786−10790. (b) Tadanaga, K.; Furukawa, Y.; Hayashi, A.; Tatsumisago, M. *Adv. Mater.* **2010**, *22*, 4401−4404. (c) Takeguchi, T.; Arikawa, H.; Yamauchi, M.; Abe, R. *ECS Trans.* **2011**, *41*, 1755−1759.

(6) (a) Murray, L. J.; Dinca, M.; Long, J. R. *Chem. Soc. Rev.* **2009**, *38*, 1294−1314. (b) Rosi, N. L.; Eckert, J.; Eddaoudi, M.; Vodak, D. T.; Kim, J.; O'Keeffe, M.; Yaghi, O. M. *Science* **2003**, *300*, 1127−1129. (c) Millward, A. R.; Yaghi, O. M. *J. Am. Chem. Soc.* **2005**, *127*, 17998−17999.

(7) (a) Li, J. R.; Sculley, J.; Zhou, H. C. *Chem. Rev.* **2011**, *112*, 869−932. (b) Matsuda, R.; Kitaura, R.; Kitagawa, S.; Kubota, Y.; Belosludov, R. V.; Kobayashi, T. C.; Sakamoto, H.; Chiba, T.; Takata, M.; Kawazoe, Y.; Mita, Y. *Nature* **2005**, *436*, 238−241. (c) Shimomura, S.; Higuchi, M.; Matsuda, R.; Yoneda, K.; Hijikata, Y.; Kubota, Y.; Mita, Y.; Kim, J.; Takata, M.; Kitagawa, S. *Nat. Chem.* **2010**, *2*, 633−637.

(8) (a) Rocca, J. D.; Liu, D.; Lin, W. *Acc. Chem. Res.* **2011**, *44*, 957−968. (b) Horcajada, P.; Chalati, T.; Serre, C.; Gillet, B.; Sebrie, C.; Baati, T.; Eubank, J. F.; Heurtaux, D.; Clayette, P.; Kreuz, C.; Chang, J.-S.; Hwang, Y. K.; Marsaud, V.; Bories, P.-N.; Cynober, Luc; Gil, S.; Férey, G.; Couvreur, P.; Gref, R. *Nat. Mater.* **2010**, *9*, 172−178.

(9) (a) Lee, J. Y.; Farha, O. K.; Roberts, J.; Scheidt, K. A.; Nguyen, S. T.; Hupp, J. T. *Chem. Soc. Rev.* **2009**, *38*, 1450−1459. (b) Seo, J. S.; Whang, D.; Lee, H.; Jun, S. I.; Oh, J.; Jeon, Y. J.; Kim, K. *Nature* **2000**, *404*, 982−986. (c) Hasegawa, S.; Horike, S.; Matsuda, R.; Furukawa, S.; Mochizuki, K.; Kinoshita, Y.; Kitagawa, S. *J. Am. Chem. Soc.* **2007**, *129*, 2607−2614.

(10) (a) Kurmoo, M. *Chem. Soc. Rev.* **2009**, *38*, 1353−1379. (b) Tamaki, H.; Zhong, Z. J.; Matsumoto, N.; Kida, S.; Koikawa, M.; Achiwa, N.; Hashimoto, Y.; Ōkawa, H. *J. Am. Chem. Soc.* **1992**, *114*, 6974−6979. (c) Tomono, K.; Tsunobuchi, Y.; Nakabayashi, K.; Ohkoshi, S. *Inorg. Chem.* **2010**, *49*, 1298−1300.

(11) (a) Takaishi, S.; Hosoda, M.; Kajiwara, T.; Miyasaka, H.; Yamashita, M.; Nakanishi, Y.; Kitagawa, Y.; Yamaguchi, K.; Kobayashi, A.; Kitagawa, H. *Inorg. Chem.* **2009**, *48*, 9048−9050. (b) Otsubo, K.; Kobayashi, A.; Kitagawa, H.; Hedo, M.; Uwatoko, Y.; Sagayama, H.; Wakabayashi, Y.; Sawa, H. *J. Am. Chem. Soc.* **2006**, *128*, 8140−8141. (c) Fuma, Y.; Ebihara, M.; Kutsumizu, S.; Kawamura, T. *J. Am. Chem. Soc.* **2004**, *126*, 12238−12239.

(12) (a) Sadakiyo, M.; Yamada, T.; Kitagawa, H. *J. Am. Chem. Soc.* **2009**, *131*, 9906−9907. (b) Ōkawa, H.; Sadakiyo, M.; Yamada, T.; Maesato, M.; Ohba, M.; Kitagawa, H. *J. Am. Chem. Soc.* **2013**, *135*, 2256−2262. (c) Sadakiyo, M.; Ōkawa, H.; Shigematsu, A.; Ohba, M.; Yamada, T.; Kitagawa, H. *J. Am. Chem. Soc.* **2012**, *134*, 5472−5475. (d) Nagao, Y.; Ikeda, R.; Kanda, S.; Kubozono, Y.; Kitagawa, H. *Mol. Cryst. Liq. Cryst.* **2002**, *379*, 89−94. (e) Hurd, J. A.; Vaidhyanathan, R.; Thangadurai, V.; Ratcliffe, C. I.; Moudrakovski, I. M.; Shimizu, G. K. H. *Nat. Chem.* **2009**, *1*, 705−710. (f) Taylor, J. M.; Mah, R. K.; Moudrakovski, I. L.; Ratcliffe, C. I.; Vaidhyanathan, R.; Shimizu, G. K. H. *J. Am. Chem. Soc.* **2010**, *132*, 14055−14057. (g) Bureekaew, S.; Horike, S.; Higuchi, M.; Mizuno, M.; Kawamura, T.; Tanaka, D.; Yanai, N.; Kitagawa, S. *Nat. Mater.* **2009**, *8*, 831−836. (h) Umeyama, D.; Horike, S.; Inukai, M.; Hijikata, Y.; Kitagawa, S. *Angew. Chem., Int. Ed.* **2011**, *50*, 1−5. (i) Ohkoshi, S.; Nakagawa, K.; Tomono, K.; Imoto, K.; Tsunobuchi, Y.; Tokoro, H. *J. Am. Chem. Soc.* **2010**, *132*, 6620−6621. (j) Pardo, E.; Train, C.; Gontard, G.; Boubekeur, K.; Fabelo, O.; Liu, H.; Dkhil, B.; Lloret, F.; Nakagawa, K.; Tokoro, H.; Ohkoshi, S.; Verdaguer, M. *J. Am. Chem. Soc.* **2011**, *133*, 15328−15331. (k) Sahoo, S. C.; Kundu, T.; Banerjee, R. *J. Am. Chem. Soc.* **2011**, *133*, 17950−17958. (l) Jeong, N. C.; Samanta, B.; Lee, C. Y.; Farha, O. K.; Hupp, J. T. *J. Am. Chem. Soc.* **2012**, *134*, 51−54. (m) Xu, G.; Otsubo, K.; Yamada, T.; Sakaida, S.; Kitagawa, H. *J. Am. Chem. Soc.* **2013**, *135*, 7438−7441.

(13) Tuckerman, M. E.; Marx, D.; Parrinello, M. *Nature* **2002**, *417*, 925−929.

(14) (a) Park, K. S.; Ni, Z.; Cote, A. P.; Choi, J. Y.; Huang, R.; Uribe-Romo, F. J.; Chae, H. K.; O'Keeffe, M.; Yaghi, O. M. *Proc. Natl. Acad. Sci. U.S.A.* **2006**, *103*, 10186−10191. (b) Phan, A.; Doonan, C. J.; Uribe-Romo, F. J.; Knobler, C. B.; O'Keeffe, M.; Yahghi, O. M. *Acc. Chem. Res.* **2010**, *43*, 58−67. (c) Cravillon, J.; Nayuk, R.; Springer, S.; Feldhoff, A.; Huber, K.; Wiebcke, M. *Chem. Mater.* **2011**, *23*, 2130−2141. (d) Küsgens, P.; Rose, M.; Senkovska, I.; Fröde, H.; Henschel, A.; Siegle, S.; Kaskel, S. *Microporous Mesoporous Mater.* **2009**, *120*, 325−330.

(15) Low, J. J.; Benin, A. I.; Jakubczak, P.; Abrahamian, J. F.; Faheem, S. A.; Willis, R. R. *J. Am. Chem. Soc.* **2009**, *131*, 15834−15842.

(16) Alston, T. A. *Anesth. Analg.* **2003**, *96*, 622−625.

(17) Karagiaridi, O.; Lalonde, M. B.; Bury, W.; Sarjeant, A. A.; Farha, K. O.; Hupp, J. T. *J. Am. Chem. Soc.* **2012**, *134*, 18790−18796.

(18) (a) Takata, M.; Nishibori, E.; Sakata, M. *Z. Kristallogr.* **2001**, *216*, 71−86. (b) Kato, K.; Hirose, R.; Takemoto, M.; Ha, S.; Kim, J.; Higuchi, M.; Matsuda, R.; Kitagawa, S.; Takata, M. *AIP Conf. Proc.* **2010**, *1234*, 875−878.

(19) (a) Higuchi, M.; Tanaka, D.; Horike, S.; Sakamoto, H.; Nakamura, K.; Takashima, Y.; Hijikata, Y.; Yanai, N.; Kim, J.; Kato, K.; Kubota, Y.; Takata, M.; Kitagawa, S. *J. Am. Chem. Soc.* **2009**, *131*, 10336−10337. (b) Sadakiyo, M.; Yamada, T.; Kitagawa, H. *J. Am. Chem. Soc.* **2011**, *133*, 11050−11053.

(20) Agmon, N. *Chem. Phys. Lett.* **1995**, *244*, 456−462.

(21) Atkins, P. W. *Physical Chemistry*, 6th ed.; Oxford University Press: Oxford, U.K., 1998; pp 740−741.

(22) Agmon, N. *Chem. Phys. Lett.* **2000**, *319*, 247−252.